International Journal of Information, Control and Computer Sciences
ISSN: 2517-9942
Vol:9, No:2, 2015

3D Objects Indexing with a Direct and Analytical Method for Calculating the Spherical Harmonics Coefficients

S. Hellam, Y. Oulahrir, F. El Mounchid, A. Sadiq, S. Mbarki

***Abstract*—**In this paper, we propose a new method for three-dimensional object indexing based on D.A.M.C-S.H.C descriptor (Direct and Analytical Method for Calculating the Spherical Harmonics Coefficients). For this end, we propose a direct calculation of the coefficients of spherical harmonics with perfect precision. The aims of the method are to minimize, the processing time on the 3D objects database and the searching time of similar objects to a request object.

Firstly we start by defining the new descriptor using a new division of 3-D object in a sphere. Then we define a new distance which will be tested and prove his efficiency in the search for similar objects in the database in which we have objects with very various and important size.

***Keywords*—**3D Object indexing, 3D shape descriptor, spherical harmonic, 3D Object similarity.

I. Introduction

WITH technological developments, three-dimensional objects conquered the majority of industries, include: video games, automotive industry, modeling and the development of 3D scanners, the architecture and bio-medical.

The rapid increase in this domain has asked to establish new tools to research and navigate in large 3D databases.

The goal of the 3D indexing is to describe compactly a 3D object shape. To do this, shape descriptors are used to obtain vectors features or 3D objects signatures that serve as a key in objects retrieval.

The spherical harmonic basis is like the Fourier basis but defined on the surface of a sphere, it's a very important tool to evaluate convolutions in one or two dimensional spaces. Many searches on computer graphics [1]-[5] have already using spherical harmonics, but this base have just recently become feasible to be used in real time computer graphics.

In this article (is the continuity of our work [6]), we will develop a new Method of Calculation of the Spherical Harmonics Coefficients with Direct and Analytical procedure named D.A.M.C-S.H.C.

For similarity between 3D objects, we then a new distance based on spherical harmonic coefficients. Finally, we have tested this distance on 3D objects for a medium and high density.

This paper is organized in the following way: Section II gives a brief survey of previous work. Next the proposed method for determination of Spherical Harmonics Coefficients is explained. The following section presents practical examples. Finally the conclusions point out the limitations and some perspectives.

S. Hellam is with LABO LARIT, Faculty of science, Ibn tofail University Morocco (phone: +212672498117; e-mail: hellamsaid@gmail.com).

Y. Oulahrir is with office of vocational training and job promotion, (phone: +212669790756; e-mail: oulahrir.ntic2@gmail.com).

F. El Mounchid is with the Ministry of Education (e-mail: elmounchid@yahoo.fr).

A. Sadiq and S. Mbarki are with Ibn Tofail University (e-mail: sadiq.alim@gmail.com, mbarkisamir@hotmail.com).

II. State of Art

In order to solve the problem of data treatment: storing, editing and manipulating, very powerful programs were developed for importing the data files and exporting them in well-standardized formats, like IGES, DXF for CAD applications and VRML for [7].

To evaluate the efficiency of the descriptor, the properties of invariance are required to eliminate differences due to translation, rotation and variation of scale.

The properties of invariance are required to eliminate differences due to rotation, translation and magnification. To avoid of these dependencies, we shall normalize the models by using the center of mass for translation, the root of the average square radius for scale and principal axis for rotation [8] , [9].

The literature provides a lot of various 3D shape descriptors, describing geometric as well as topological properties of 3D shapes grouped in four classes:

- Global shape descriptors [4], [5] and [8]-[14];
- Local descriptors [15];
- Graph based methods [10], [16] and [17];
- Geometric methods based on 2D views of 3D models [18], [19].

The team of Leipzig has also proposed to apply a Fourier transform on the sphere S_2 [20] by applying the proposed spherical harmonic.

Then, to overcome the problem of invariance to rotation, the Princeton team proposed to apply the spherical harmonic decomposition of spherical functions defined by the intersection of the surface of the 3D object with a set of concentric spheres [11].

The spherical harmonics method of Princeton's team [11] gave better results in their database than their previous descriptor (distribution of 2D form). However, it is based on a 3D model voxelization, therefore depends on the level of resolution of the voxelization, and resulting in a loss of detail in the description of the object.

That is why [20] proposing to apply the method directly on

3D meshes with new spherical functions. The results they obtained on their database with their method are less time consuming.

However, results of [21] also show that the encoded information does not really make specific requests on shapes, the main limitation is the number of concentric spheres and the number of coefficients harmonics remaining may be too low. The authors choose in practice 32 concentric spheres and 16 harmonics per sphere. Thus, their descriptor has 32*16= 512 coefficients.

Different 3D shape description methods have been proposed in this research area. Teams [22] have realized a comparative study of 3D retrieval algorithms [11], [23]. Those algorithms can be clustered into two main families: 2D/3D approaches and 3D/3D approaches. The descriptor using 2D/3D approaches, the description model is obtained through different 2D projections of the 3D shape, whereas for the descriptor using 3D/3D approaches, the description model is obtained from the 3D information directly extracted from the 3D shape [24].

Peijiang Liu et al. [25] have represented 3D face models in a canonical representation, namely Spherical Depth Map (SDM). Then, considering the predictive contribution of each SHF feature, especially in the presence of facial expression and occlusion, feature selection methods are used to improve the predictive performance and provide faster and more cost-effective predictors.

III. Spherical Harmonic Method

A. Invariant 3D Shape Descriptors

It is designed to normalize the different objects in a coordinate in order to ensure unique representation. The properties of invariance are required to eliminate differences due to rotation, translation and the variation of scale. To avoid these dependencies, we shall normalize the models by using the center of mass for translation, the root of the average square radius for scale and principal axis for rotation [8], [14] and [26].

B. Representation of Spherical Harmonics

The gradient in spherical coordinates is [27]:

$$\vec{\nabla} = \frac{\partial}{\partial\theta}\vec{e}\,r + \frac{1}{r}\frac{\partial}{\partial\theta}\vec{e}\,\theta + \frac{\partial}{\partial\varphi}\vec{e}\,\varphi \tag{1}$$

The Laplacian of a function f:

$$\nabla^2 f = \frac{1}{r^2}\frac{\partial}{\partial r}\left(r^2\frac{\partial f}{\partial r}\right) + \frac{1}{r^2\sin\theta}\frac{\partial}{\partial\theta}\left(\sin(\theta)\frac{\partial f}{\partial\theta}\right) + \frac{1}{r^2\sin(\theta)}\frac{\partial^2 f}{\partial\varphi^2} \tag{2}$$

$$Y_l^m(\theta,\varphi) = \sqrt{\frac{2l+(l-m)!}{4\pi(l+m)!}}P_l^m(\cos(\theta))e^{im\varphi} \tag{3}$$

P_l^m is the Legendre polynomial associated of *l* degree and *m order*, θ varies between $[0,\pi]$ and φ varies between $[0,2\pi]$ [27].

$$P_l^m(x) = \frac{(-1)^m}{2^l l!}(1-x^2)^{\frac{m}{2}}\frac{d^{l+m}}{dx^{l+m}}(x^2-1)^l \tag{4}$$

Spherical harmonic decomposition: $\left\{Y_l^m / m \in \mathrm{Z}\ et\ l \in \mathrm{N}\right\}$ Orthonormal basis in the Hilbert space L^2 (S^2) with S^2 unit sphere [24].

$$\int_0^{2\pi}\int_0^{\pi} Y_l^m(\theta,\varphi)\overline{Y}_{l'}^{m'}(\theta,\varphi)\sin(\theta)d\theta\,d\varphi = \delta_{ll'}\delta_{mm'} \tag{5}$$

δ_{ij} is Symbol of Kronecker, where:

$$\delta_{ij} = \begin{cases} 1 & \text{if } i = j \\ 0 & \text{if } i \neq j \end{cases} \tag{6}$$

We have:

$$-\Delta Y_l^m(\theta,\varphi) = l(l+1)Y_l^m(\theta,\varphi) \tag{7}$$

and:

$$-i\frac{\partial}{\partial\varphi}Y_l^m = mY_l^m \tag{8}$$

The graphical representation:

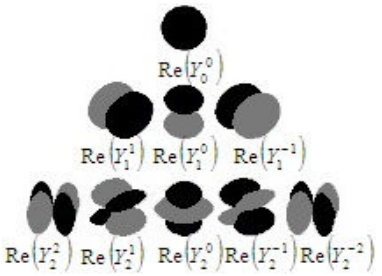

Fig. 1 Representation of the real parts of spherical harmonics for $l = 2$ and $-l \le m \le l$. The black color represents positive values and the gray color represents negative values

Representative surfaces are bumpy spheres: bumps correspond to the parts where $Y_l^m(\theta,\varphi)$ positive, dips are corresponding to the parts where $Y_l^m(\theta,\varphi)$ is negative, θ and φ describe the interval $[0,\pi]$ and $[0,2\pi]$. The parameters l and m are defined by [27]:

- m : circles along the meridian, an iso-longitude.
- $l-m$ *:* circles in a parallel, an iso-latitude.

Spherical harmonic decomposition (S.H.D):

Let $f(\theta,\varphi)$ be a harmonic function defined on the closed interval $[-1,1]$ [24].

$$f(\theta,\varphi) = \sum_{l=0}^{\infty}\sum_{m=-l}^{l} C_{lm}Y_l^m(\theta,\varphi) \tag{9}$$

$C_{l,m}$ are the harmonic coefficients of order (l,m).

Hermitian scalar product:

$$\langle f,g\rangle = \frac{1}{4\pi}\iint_{S^2} f^* g \sin(\theta)\, d\theta\, d\varphi \tag{10}$$

where f^* : is the complex conjugate of f indeed [27]:

$$C_{l;m} = \langle Y_l^m, f\rangle = (-1)^m \sqrt{\frac{2l+(l-m)!}{4\pi(l+m)!}} \cdot \int_0^{2\pi}\int_0^{\pi} \mathrm{f} \times P_l^m(\cos(\theta)) e^{-im\varphi} \sin(\theta)\, d\theta\, d\varphi \tag{11}$$

We have:

$$C_{l,-m} = (-1)^m C_{l,m}^* \tag{12}$$

$C_{l,m}^*$: is the complex conjugate of $C_{l,m}$.

From (12), it is sufficient to calculate the coefficients $C_{l,m}$ for m positive, so that reduced half of the computation time. The dimension of the $L^2(S^2)$ space is $2l+1$ ξ : is the set of points which create the 3D object. The indicator function:

$$\chi(r,\theta,\varphi) = \begin{cases} 1 & \text{if} \quad M \in \xi_S \\ 0 & \text{if} \quad M \notin \xi_S \end{cases} \tag{13}$$

where ξ_S is the set of points belonging to the object and the sphere (S^2) with radius r. Thus: $\xi_S = \xi \cap (S^2)$

C. Mathematical Development of D.A.M.C-S.H.C Descriptor

We calculate the coefficients of the spherical harmonics for different cases of m:

- $m = 0$
- $0 < m < l$
- $m = l$

There are three possible cases for the existence of points M regarding to ξ_S :

$$d = r_i - r \tag{14}$$

$$\begin{cases} d > 0 \quad \text{or} \quad d < 0 \quad \Rightarrow M \notin \xi_S \\ d = 0 \quad \Rightarrow \quad M \in \xi_S \end{cases} \tag{15}$$

We consider an infinitely small area A_k defined by a spherical square offside $2r\varepsilon$, on the sphere S^2 of radius r and center M_k . This area is represented in Fig. 2.

$$\varphi_k = \arctan(\frac{y_k}{x_k}) \tag{16}$$

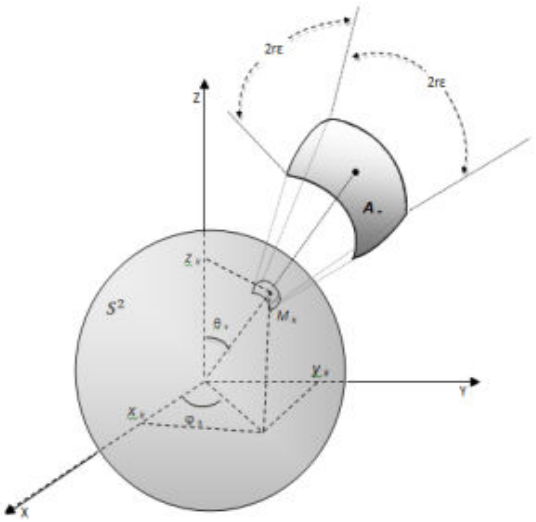

Fig. 2 Representative Schema of A_k area on the sphere S^2 of radius r

$$\theta_k = \arccos\left(\frac{z_k}{\sqrt{x_k^2 + y_k^2 + z_k^2}}\right) \tag{17}$$

$$C_{l,m} = (-1)^m \sqrt{\frac{2l+(l-m)!}{4\pi(l+m)!}} \cdot \int_{\varphi_k-\varepsilon}^{\varphi_k+\varepsilon} e^{-im\varphi} d\varphi \int_{\theta_k-\varepsilon}^{\theta_k+\varepsilon} P_l^m(\cos(\theta))\sin(\theta)\, d\theta \tag{18}$$

We choose ε infinitely small where $0 \le \theta \le \pi$ and $0 \le \varphi \le 2\pi$:

$$C_{l;m} = (-1)^m \sqrt{\frac{2l+(l-m)!}{4\pi(l+m)!}} \times I_{\varphi_{k,\varepsilon}} \times I_{\theta_{k,\varepsilon}} \tag{19}$$

with

$$I_{\varphi k,\varepsilon} = \int_{\varphi_k-\varepsilon}^{\varphi_k+\varepsilon} e^{-im\varphi} d\varphi \tag{20}$$

and

$$I_{\theta_{k,\varepsilon}} = \int_{\theta_k-\varepsilon}^{\theta_k+\varepsilon} P_l^m(\cos(\theta))\ \sin(\theta) d\theta \tag{21}$$

Case**:** $m = 0$

Using a variable change: $t = \cos\theta$, after integration $I_{\theta_{k,\varepsilon}}$ is written like a formula [28]:

$$I_{\theta_{k,\varepsilon}} = \left[\frac{P_{l+1}(t) - P_{l-1}(t)}{2l+1}\right]_{\cos(\theta_k-\varepsilon)}^{\cos(\theta_k+\varepsilon)} \tag{22}$$

Finally, we find a coefficient of spherical harmonic decomposition (S.H.D) expressed by:

$$C_{l,0}^{k,\varepsilon} = \frac{-\varepsilon}{2l+1}\sqrt{\frac{2l+l!}{\pi\, l!}} \times \begin{Bmatrix} P_{l+1}(\cos(\theta_k+\varepsilon)) + P_{l-1}(\cos(\theta_k-\varepsilon)) \\ -P_{l+1}(\cos(\theta_k-\varepsilon)) - P_{l-1}(\cos(\theta_k+\varepsilon)) \end{Bmatrix} \quad (23)$$

Case: $1 \le m \le l-1$

From where (20):

$$I_{\varphi_{k,\varepsilon}} = \frac{2e^{-im\varphi_k}}{m}\sin(m\varepsilon) \quad (24)$$

The calculation of $I_{\theta_{k,\varepsilon}}$ (21) and according to the formula [29]:

$$P_l^m(\cos(\theta)) = (-1)^m(\sin(\theta))^m \frac{d^m P_l(\cos(\theta))}{d\cos^m(\theta)} \quad (25)$$

we set $D = \frac{d}{dz}$ and we have [30]

$$D^m P_l(z) = \frac{(-1)^m(l+m)!}{2^m(l-m)!m!}\, {}_2F_1(m-l, l+m+1; m+1; \frac{1-z}{2}) \quad (26)$$

where: $F(a,b;c;z)$ is the hypergeometric function which is defined by [31] :

$${}_2F_1(a,b;c;z) = \sum_{j=0}^{\infty} \frac{(a)_j (b)_j}{(c)_j\, j!} z^j = F(a,b;c;z) \quad (27)$$

and $(a)_j$: Pochhammer symbol [32].

$$(a)_j = a(a+1)(a+2).....(a+j-1) = \frac{\Gamma(a+j)}{\Gamma(a)} \quad (28)$$

This series converges for $|z| < 1$[33].

$${}_2F_1(a,b;c;x) = \frac{\Gamma(c)}{\Gamma(b)\Gamma(c-b)}\int_0^1 t^{b-1}(1-t)^{c-b-1}(1-xt)^{-a}dt \quad (29)$$

$${}_2F_1(a,b;c;x) = \frac{\Gamma(c)}{\Gamma(b)\Gamma(c-b)}\sum_{k=0}^{\infty}\frac{\Gamma(a+k)\Gamma(b+k)}{\Gamma(c+k)\,k!}x^k \quad (30)$$

where $\Gamma(z)$ is the Gamma of Euler function which is defined by [34]:

$$\Gamma(z) = \int_0^{\infty} e^{-t}t^{z-1}dt = (z-1)! \quad (31)$$

and $z \neq -1,-2,-3,.....$ We have:

$$\Gamma(z+1) = z\Gamma(z) \quad (32)$$

$$\Gamma\left(\frac{1}{2}\right) = \sqrt{\pi} \quad (33)$$

$$\Gamma\left(n+\frac{1}{2}\right) = \frac{n!!}{2^n}\sqrt{\pi} \quad (34)$$

where

- $n!! = 1.3.5.....(n-2)n$ if n is odd
- $n!! = 2.4.6.....(n-2)n$ if n is even
- $n!! = 1$ if $n = -1$ or $n = 0$

The derivative n order of the hypergeometric function $F(a,b;c;z)$ can be expressed by [30], [33]:

$$\frac{d^n}{dz^n}F(a,b;c;z) = \frac{(a)_n(b)_n}{(c)_n}F(a+n,b+n;c+n;z) \quad (35)$$

If $z = \cos\theta$ we have $D = \frac{d}{d\cos\theta}$ from where the expression of $I_{\theta_{k,\varepsilon}}$:

$$I_{\theta_{k,\varepsilon}} = (-1)^m \int_{\theta_k-\varepsilon}^{\theta_k+\varepsilon} (\sin(\theta))^{m+1} D^m(P_l(\cos(\theta)))d\theta \quad (36)$$

Combining (25) and (26) the expression $I_{\theta_{k,\varepsilon}}$ is written with:

$$I_{\theta k,\varepsilon} = \frac{(l+m)!}{2^m(l-m)!m!} \times \int_{\theta_k-\varepsilon}^{\theta_k+\varepsilon} (\sin(\theta))^{m+1} F\left(m\text{-}l, l+m+1; m+1; \frac{1-\cos(\theta)}{2}\right)d\theta \quad (37)$$

With a change of variable $t = \sin^2\left(\frac{\theta}{2}\right)$ the expression of $I_{\theta k,\varepsilon}$ (37) becomes:

$$I_{\theta_{k,\varepsilon}} = \frac{2(l+m)!}{(l-m)!\,m!} \times \int_{\sin^2\left(\frac{\theta_k-\varepsilon}{2}\right)}^{\sin^2\left(\frac{\theta_k+\varepsilon}{2}\right)} (t\times(1-t))^{\frac{m}{2}} F\left(m\text{-}l, l+m+1; m+1; t\right)dt \quad (38)$$

By using the relationship of chasles:

$$I_{\theta_{k,\varepsilon}} = \frac{2(l+m)!}{(l-m)!\,m!} \times \left[\int_0^{\sin^2\left(\frac{\theta_k+\varepsilon}{2}\right)} (t\times(1-t))^{\frac{m}{2}} F\left(m\text{-}l, l+m+1; m+1; t\right)dt - \int_0^{\sin^2\left(\frac{\theta_k-\varepsilon}{2}\right)} (t\times(1-t))^{\frac{m}{2}} F\left(m\text{-}l, l+m+1; m+1; t\right)dt \right] \quad (39)$$

We put and define J by:

$$J=\int_0^x t^{\frac{m}{2}}(1-t)^{\frac{m}{2}}F(m\text{-}l,l+m+1;m+1;t)\,dt \tag{40}$$

The development of $F(m\text{-}l,l+m+1;m+1;t)$ series gives:

$$J=\int_0^x t^{\frac{m}{2}}(1-t)^{\frac{m}{2}}\left(\sum_{j=0}^{l-m}\frac{(m-l)_j(l+m+1)_j}{(m+l)_j\,j!}t^j\right)dt \tag{41}$$

$$J=\sum_{j=0}^{l-m}\frac{(m-l)_j(l+m+1)_j}{(m+l)_j\,j!}\int_0^x t^{\frac{m}{2}+j}(1-t)^{\frac{m}{2}}dt \tag{42}$$

with:

$$J=\sum_{j=0}^{l-m}\frac{(m-l)_j(l+m+1)_j}{(m+l)_j\,j!}B_x\left(\frac{m}{2}+j+1;\frac{m}{2}+1\right) \tag{43}$$

and:

$p>0$, $q>0$ and $0\le x\le 1$

$B_x(p,q)$ is the Beta incomplete function [30], [34].

$$B_x(p,q)=\int_0^x t^{p-1}(1-t)^{q-1}dt \tag{44}$$

For $x=1$ we have:

$$B_1(p,q)=\frac{\Gamma(p)\Gamma(q)}{\Gamma(p+q)} \tag{45}$$

Refer to [30], we have:

$$B_x(p,q)=\frac{x^p}{p}\,{}_2F_1(p,1-q;1+p;x) \tag{46}$$

J is written in:

$$J=\sum_{j=0}^{l-m}\frac{(m-l)_j(l+m+1)_j}{(m+l)_j\left(\frac{m}{2}+1+j\right)j!}x^{\frac{m}{2}+1+j}\times {}_2F_1\left(\frac{m}{2}+j+1,-\frac{m}{2};\frac{m}{2}+j+2;x\right) \tag{47}$$

According to (39) and (47), $I_{\theta_{k,\varepsilon}}$ can be written in:

$$I_{\theta_{k,\varepsilon}}=\frac{2(l+m)!}{(l-m)!m!}\times \left\{\sum_{j=0}^{l-m}\left(\frac{(m-l)_j(l+m+1)_j}{(m+l)_j(\frac{m}{2}+1+j)j!}\times \left[\left(\sin\left(\frac{\theta_k+\varepsilon}{2}\right)\right)^{m+2+2j}{}_2F_1\left(\frac{m}{2}+1+j,-\frac{m}{2};\frac{m}{2}+2+j;\sin^2\left(\frac{\theta_k+\varepsilon}{2}\right)\right)\right]-\left[\left(\sin\left(\frac{\theta_k-\varepsilon}{2}\right)\right)^{m+2+2j}{}_2F_1\left(\frac{m}{2}+1+j,-\frac{m}{2};\frac{m}{2}+2+j;\sin^2\left(\frac{\theta_k-\varepsilon}{2}\right)\right)\right]\right)\right\} \tag{48}$$

From where coefficients $C_{l,m}^{k,\varepsilon}$ were calculated for $1\le m\le l-1$ we have:

$$C_{l,m}^{k,\varepsilon}=\frac{2(-1)^m\sqrt{(l+m)!(2l+(l-m)!)}}{\sqrt{\pi}m(l-m)!m!}\sin(m\varepsilon)e^{-im\varphi_k}\times \left\{\sum_{j=0}^{l-m}\left(\frac{(m-l)_j(l+m+1)_j}{(m+l)_j(\frac{m}{2}+1+j)j!}\times \left[\left(\sin\left(\frac{\theta_k+\varepsilon}{2}\right)\right)^{m+2+2j}{}_2F_1\left(\frac{m}{2}+1+j,-\frac{m}{2};\frac{m}{2}+2+j;\sin^2\left(\frac{\theta_k+\varepsilon}{2}\right)\right)\right]-\left[\left(\sin\left(\frac{\theta_k-\varepsilon}{2}\right)\right)^{m+2+2j}{}_2F_1\left(\frac{m}{2}+1+j,-\frac{m}{2};\frac{m}{2}+2+j;\sin^2\left(\frac{\theta_k-\varepsilon}{2}\right)\right)\right]\right)\right\} \tag{49}$$

Case $m=l$

We have:

$$I_{\theta_{k,\varepsilon}}=\frac{(-1)^l(2l)!}{2^l\,l!}\int_{\theta_k-\varepsilon}^{\theta_k+\varepsilon}\left(1-\cos^2(\theta)\right)^{\frac{l}{2}}\sin(\theta)\,d\theta \tag{50}$$

$I_{\theta_{k,\varepsilon}}$ is calculated by a change of variable $t=\sin\left(\frac{\theta}{2}\right)$

We obtain:

$$I_{\theta_{k,\varepsilon}}=\frac{(-1)^l(2l)!}{2^{\frac{l}{2}-2}\,l!}\int_{\sin\left(\frac{\theta_k-\varepsilon}{2}\right)}^{\sin\left(\frac{\theta_k+\varepsilon}{2}\right)}t^{l+1}dt \tag{51}$$

From where:

$$I_{\theta_{k,\varepsilon}}=\frac{(-1)^l(2l)!}{2^{\frac{l}{2}-2}(l+2)!}\left[\left(\sin\left(\frac{\theta_k+\varepsilon}{2}\right)\right)^{l+2}-\left(\sin\left(\frac{\theta_k-\varepsilon}{2}\right)\right)^{l+2}\right] \tag{52}$$

and

$$C_{l,l}^{k,\varepsilon}=\frac{\sqrt{(2l)!(2l+1)}}{\sqrt{\pi}\,2^{\left(\frac{l-4}{2}\right)}l(l+2)l!}\sin(l\varepsilon)\,e^{-il\varphi_k}\times\left[\left(\sin\left(\frac{\theta_k+\varepsilon}{2}\right)\right)^{l+2}-\left(\sin\left(\frac{\theta_k-\varepsilon}{2}\right)\right)^{l+2}\right] \tag{53}$$

The coefficients of S.H.D $C_{l,m}^{r,k,\varepsilon}$ are given with:

$$C_{l,m}^{r,k,\varepsilon} = r_k C_{l,m}^{k,\varepsilon} \tag{54}$$

where: $0 \le k \le N$ and N is the number of points form the 3D object.

$$N = card(\xi) \tag{55}$$

$$H = \begin{bmatrix} C_{l,-l}^{1} & \cdots & C_{l,-l+j}^{1} & \cdots & C_{l,l}^{1} \\ \vdots & \ddots & \vdots & \cdots & \vdots \\ C_{l,-l}^{i} & \cdots & C_{l,-l+j}^{i} & \cdots & C_{l,l}^{i} \\ \vdots & \vdots & \vdots & \ddots & \vdots \\ C_{l,-l}^{N} & \cdots & C_{l,-l+j}^{N} & \cdots & C_{l,l}^{N} \end{bmatrix} \tag{56}$$

This matrix is represented by a $2l+1$ rows and N columns, where N is the number of points which represent the 3D object.

Each row R_k characterize the point P_k by the $2l+1$ coefficients of spherical harmonic $C_{l,m}^{k}$, where $1 \le k \le N$ and $-l \le m \le l$.

In each column C_m we calculate the different coefficients $C_{l,m}^{k}$ for all points defining the object.

D.Measurement of Similarity Based on New Distance Using Spherical Harmonic Coefficients.

We define for same value l the coefficient F_i:

$$F_i = \left(\frac{\sum_{k=1}^{N_i} \left(\sum_{m=-l}^{l} \left| C_{l,m}^{k} \right| \right)}{(2l+1) \times N_i} \right)^{\frac{1}{N_i}} \tag{57}$$

where N_i is the number of points in O_i object. F_i represents the arithmetic average of all the spherical harmonic coefficients of the matrix H.

$$D = \left| F_i - F_j \right| \tag{58}$$

where i and j indicate the objects F_i and F_j respectively.

Special case: For $N \longrightarrow +\infty$; we have:

$$\lim_{x \to +\infty} \left(\frac{1}{x} \right)^{\frac{1}{x}} = 1$$

Thus:

$$\lim_{N \to +\infty} F_i = 1 = F_\infty$$

For two objects O_1 and O_2, where $N_2 \to +\infty$

$$D = \left| 1 - F_1 \right| \tag{59}$$

So we can say that the object O_2 is transparent with respect to the object O_1.

IV. Experiments and Results

Experience 1

For testing the new distance of similarity indicated in (15) for 3D objects, we have chosen two classes of objects: class-1, and class-2 as we show in Figs. 3 and 4.

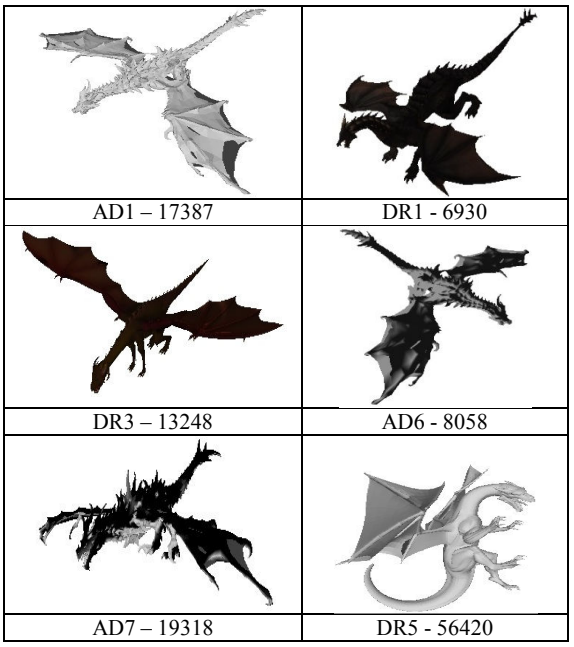

Fig. 3 Classes of objects: Dragons objects class -1-

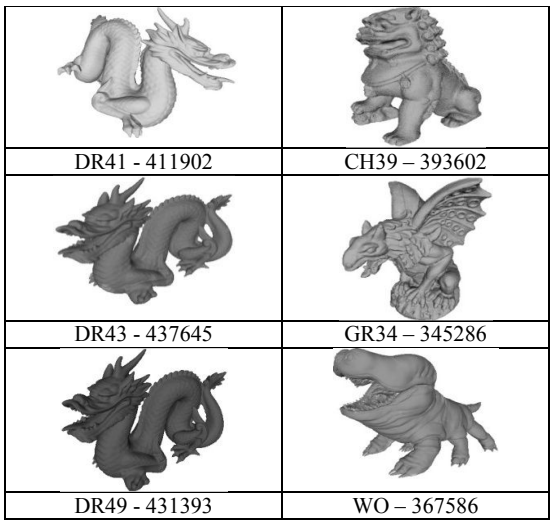

Fig. 4 Classes of objects: Dragons objects class -2-

TABLE I
NUMBER OF POINTS FOR EACH OBJECT IN THE DRAGONS CLASS -1-

Object	Number of Points
AD1	17387
AD6	8058
AD7	19318
DR1	6930
DR3	13248
DR5	56420

In order to test the distance of similarity chosen, we compare an object to the other objects in the same class.

Tables I, II show the number of points for each object per class type.

TABLE II
NUMBER OF POINTS FOR EACH OBJECT IN THE DRAGONS CLASS -2-

Object	Number of Points
DR41	411902
DR43	437645
DR49	431393
CH39	393602
GR34	345286
WO36	367586

TABLE III
MEASUREMENT OF SIMILARITY BETWEEN THE DRAGON ADUIN AND THE OTHER OBJECTS IN THE CLASS-1

Value l	AD6-AD1	AD6-AD7	AD6-DR1	AD6-DR3	AD6-DR5
1	3.305954905074154E-003	3.590264554174365E-003	9.572295753696623E-004	2.421133133402061E-003	5.280939292404200E-003
3	2.768404905801129E-003	3.005843966321622E-003	7.403352871099545E-004	2.013253044932185E-003	4.426004108096816E-003
5	2.695053739087453E-003	2.925533475946911E-003	6.955403071854912E-004	1.962367749979350E-003	4.323948541309477E-003
7	2.619122475505474E-003	2.841420889142658E-003	6.557661979762783E-004	1.906968870347019E-003	4.208711053520105E-003
9	2.534878784750708E-003	2.748453413279848E-003	6.166047012906716E-004	1.844118770532551E-003	4.071946160712439E-003
11	2.437864953174476E-003	2.642311505781867E-003	5.795290475081596E-004	1.772595588052378E-003	3.915617208747994E-003
13	2.331422649347388E-003	2.526438374833881E-003	5.436745087596501E-004	1.693844529034309E-003	3.744805651093603E-003
15	2.216767541035661E-003	2.402147616406026E-003	5.093505904201337E-004	1.608793193336136E-003	3.562943976550524E-003
17	2.097760244943998E-003	2.272738766633720E-003	4.755864833914239E-004	1.520709606574321E-003	3.374392032053340E-003
19	1.976792142168057E-003	2.141237732503363E-003	4.410933862454507E-004	1.431973962083301E-003	3.182216971474863E-003
21	1.854887040607834E-003	2.008736947076823E-003	4.060936549864157E-004	1.343492379555233E-003	2.987807791917688E-003
23	1.730255080244560E-003	1.873492385336859E-003	3.717857906025494E-004	1.252616916291006E-003	2.789936204921876E-003
25	1.603084740708131E-003	1.735786880675619E-003	3.379346415146995E-004	1.160034807845448E-003	2.589021071066818E-003
27	1.474489796527418E-003	1.596563832295771E-003	3.043099686662900E-004	1.066577565229220E-003	2.386180075323090E-003
29	1.345718032277177E-003	1.457093346739516E-003	2.701033787345928E-004	9.735132630244537E-004	2.182645909346825E-003
31	1.215647319647140E-003	1.315887878864533E-003	2.364614863308507E-004	8.793607412576574E-004	1.977188357445947E-003
33	1.084608810554440E-003	1.173591029916109E-003	2.027297590155847E-004	7.841975990240577E-004	1.770268860701984E-003
35	9.538617307501753E-004	1.031507144341447E-003	1.679356123748129E-004	6.894363234592089E-004	1.563269439043195E-003

TABLE IV
MEASUREMENT OF SIMILARITY BETWEEN THE DRAGON DR41 AND THE OTHER OBJECTS IN THE CLASS-2

Value l	DR41-DR49	DR41-DR43	DR41-CH39	DR41-GR34	DR41-WO36
1	6.256478437991918E-006	7.905488385630711E-006	4.464127539861027E-006	2.208274139706655E-005	1.339990143663555E-005
3	4.516360058593057E-006	5.885563846521030E-006	5.371166212736554E-006	1.988874794842555E-005	1.247291432307529E-005
5	4.390463404231333E-006	5.719463757127810E-006	5.632360222613392E-006	1.963362386631784E-005	1.229641136770755E-005
7	4.251025029324029E-006	5.534381759823262E-006	5.889699784316401E-006	1.934756712989889E-005	1.211872536146299E-005
9	4.096579828939131E-006	5.329820876898183E-006	6.080745877327400E-006	1.894371278879202E-005	1.187927174173026E-005
11	3.927127598941157E-006	5.106452089742434E-006	6.215131319130924E-006	1.843776786763417E-005	1.158344018720322E-005
13	3.745207202357796E-006	4.865271771141184E-006	6.303808396970875E-006	1.786103771278481E-005	1.124209124534940E-005
15	3.556507367952439E-006	4.615514136883697E-006	6.348503288566571E-006	1.722996673071404E-005	1.086761271346695E-005
17	3.365133392110094E-006	4.360981517473545E-006	6.356033058514264E-006	1.655885665210745E-005	1.046996455786108E-005
19	3.168351045835637E-006	4.100714684059591E-006	6.332479275640991E-006	1.585757526558867E-005	1.005405905488220E-005
21	2.968032379652239E-006	3.837452131231079E-006	6.280896274293878E-006	1.513236184803147E-005	9.624742555535033E-006
23	2.765960491108908E-006	3.570631052357608E-006	6.202584803817913E-006	1.438564662536312E-005	9.181700721341336E-006
25	2.563165794852750E-006	3.303390070865547E-006	6.098207209396514E-006	1.361907511507229E-005	8.724012278639524E-006
27	2.357476694004451E-006	3.033309564368330E-006	5.976666486047326E-006	1.283704361938954E-005	8.255986255674278E-006
29	2.150695597244435E-006	2.761897418586162E-006	5.840941298636108E-006	1.204665640732198E-005	7.778650623769439E-006
31	1.942220092603217E-006	2.489165720647108E-006	5.690714421911205E-006	1.124607931694924E-005	7.290944036642715E-006
33	1.732845937706714E-006	2.216058734378669E-006	5.524511405641383E-006	1.043535595417921E-005	6.793936035874300E-006
35	1.523088836122668E-006	1.941589959266485E-006	5.346433967895242E-006	9.617788201334617E-006	6.290540052508893E-006

Table III shows a sample of the values of the D distance calculated between Dragon Aduin and other Objects from the class-1 for values of l between 1 and 35.

Table IV shows a sample of the values of the D distance calculated between Dragon DR41 and other Objects from the class-2 for values of l between 1 and 35.

For testing the similarity distance, we draw the graph of a function D depending on the parameter l and $\varepsilon = 10^{-11}$.

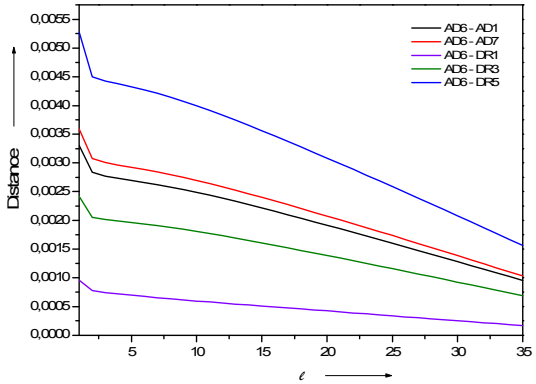

Fig. 5 Measurement of similarity between Aduin dragon AD6 and other dragons in the class -1-

Fig. 5 shows that dragons AD1and AD7 are most similar to the dragon AD6 relative to dragons DR1, DR3 and DR5. This result proves that our similarity distance provides highly reliable measurement, but not at 100%.

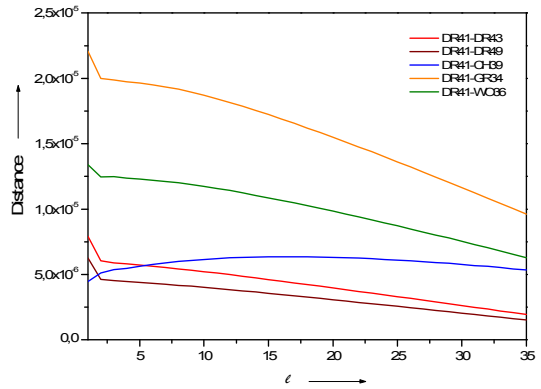

Fig. 6 Measurement of similarity between dragon DR41 and other dragons in the class -2-

Fig. 6 shows that dragon DR41 is most similar to dragons DR43 and DR49 relative to other dragons.

For DR41-DR43 and DR41-DR49, we note that the symmetry increases proportionally with l and the object is identified. By cons, for low values of l, the number of symmetries is insufficient to identify the objects. We also note that all curves are decreasing functions which show that the symmetry increases and the details of the object appear.

Experience 2

In this part of this article, to index objects with various densities of distribution, we will examine the influence of ε, where $2r\varepsilon$ is the side of the spherical square used for the integration (see Fig. 7). For this experience we choose $l = 35$, since the number of spherical harmonics and symmetry increase with l, In which case we have more details for the object. For that purpose, We draw $D = f(-\log_{10}\varepsilon)$ for values of ε varying in the interval $[10^{-20}, 10^{-1}]$.

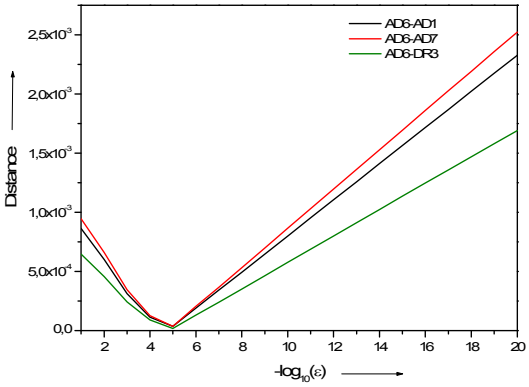

Fig. 7 The measurement of similarity between dragon AD6 and other dragons in class-1- with ε variance

Explanation of the Results:

Fig. 7 shows $D = f(-\log_{10}\varepsilon)$ passes always by a minimum $\varepsilon = 10^{-5}$, then it increases. It is due to several factors such as:

- The distribution and the density of points in the object;
- The number of points in the object.

We also note that for the value $\varepsilon = 10^{-5}$, Objects are similar because they have a very weak distance $D \approx 2.54 \times 10^{-5}$. On the other hand, when the value of ε decreases, we see that the distance increases with the number of points for various types of similar objects or not. To index well objects, the choice of ε optimal has to be in the interval $[10^{-15}, 10^{-6}]$.

For the mathematicians, the point has no dimension. However, in the IT domain, the point has dimensions, what does not allow to choose $\varepsilon = 0$: Because in our theory we integrate on a surface the center of which is a point of the object.

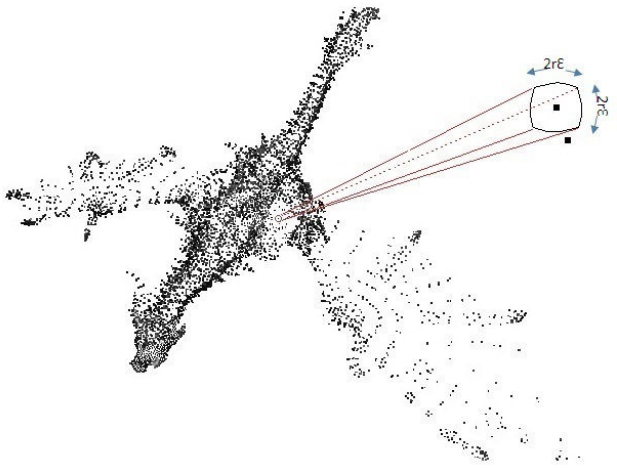

Fig. 8 Aduin dragon containing 8058 Points

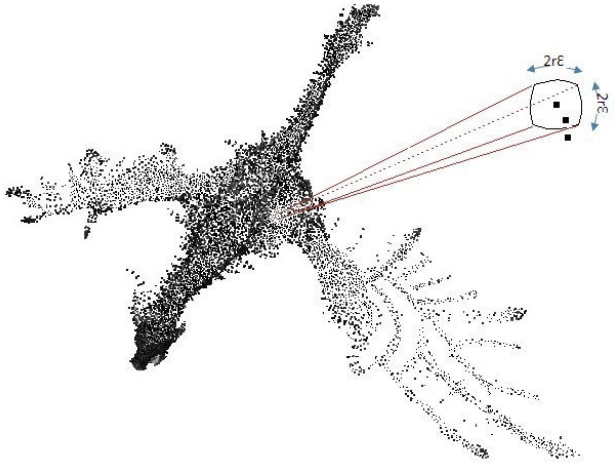

Fig. 9 Aduin dragon containing 19318 Points

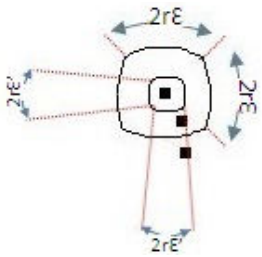

Fig. 10 The optimal choice of the spherical surface

Figs. 8-10 represent the problem of increasing the density of points for the Aduin dragon and the optimal choice of the spherical surface width $2r\varepsilon$. Therefore ε' is the optimal choice of ε parameter.

Experience 3

In the next step, we test our new descriptor on the same object with different points as shown in Fig. 10:

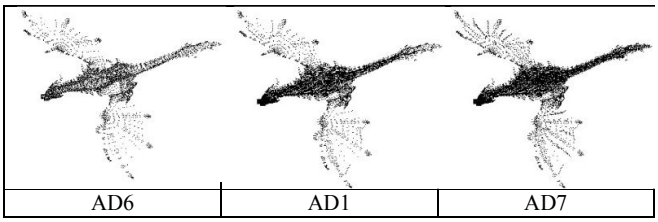

Fig. 11 The same object with different number of points

TABLE V
NUMBER OF POINTS FOR EACH OBJECT ADUIN DRAGON

Object	Number of Points
AD6	8058
AD1	17387
AD7	19318

Fig. 12 shows the existence of a low error due to augmentation of number of points for the same object. That's why we define a coefficient of relative error δ as shown in:

$$\delta = \frac{|D_1 - D_2|}{D_1} \tag{60}$$

D_1 and D_2 are respectively the distances between objects AD6 - AD7 and AD6 – AD1.

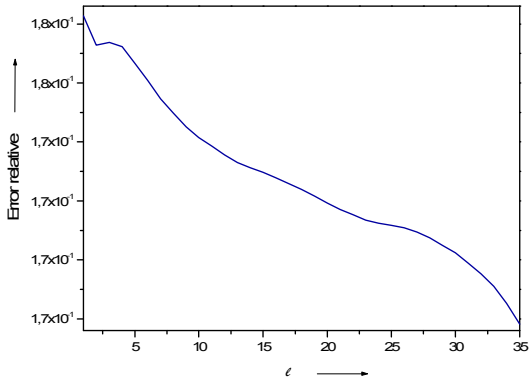

Fig. 12 Measurement of the relative error between distances AD6-AD1 and AD6-AD7

We note that the relative error decreases as increases l. Either N_1 and N_2 are respectively the number of points for objects 1 and 2. If N_1 and N_2 are different, there has:

$$N_2 = N_1 + N \quad \text{or} \quad N_2 > N_1$$

where N is the difference of points between the objects 1 and 2. F_2 becomes:

$$F_2 = \left(\frac{\sum_{k=1}^{N_1+N} \left(\sum_{m=-l}^{l} \left| C_{l,m}^{k,2} \right| \right)}{(2l+1) \times (N_1 + N)} \right)^{\frac{1}{N_1+N}} \tag{61}$$

with $C_{l,m}^{k,2}$ are the spherical harmonic coefficients of the object 2.

Special case: $N << N_1$

Since the objects 1 and 2 have the same position of the points in the space with the difference in density In this case we can consider that the spherical harmonic coefficients $C_{l,m}^{k}$ are the same that is to say:

$$C_{l,m}^{k,1} = C_{l,m}^{k,2} = C_{l,m}^{k}$$

$F_2 \approx F_1$ thus $D \approx 0$

$$F_2 = \left(\frac{\sum_{k=1}^{N_1} \left(\sum_{m=-l}^{l} \left| C_{l,m}^{k} \right| \right)}{(2l+1) \times (N_1 + N)} \right)^{\frac{1}{N_1} \frac{N}{(N_1+N)N_1}} \quad (62)$$

After mathematical development we obtain:

$$F_2 = \left(\frac{\sum_{k=1}^{N_1} \left(\sum_{m=-l}^{l} \left| C_{l,m}^{k} \right| \right)}{(2l+1) \times (N_1)} \right)^{\frac{1}{N_1}} \times \left(\frac{N_1 (2l+1)}{\sum_{k=1}^{N_1} \left(\sum_{m=-l}^{l} \left| C_{l,m}^{k} \right| \right)} \right)^{\frac{N}{N_1^2}} \quad (63)$$

we can write:

$$F_2 = F_1 \times \sigma_{12} \quad (64)$$

where σ_{12} is called correction term:

$$\sigma_{12} = \left(\frac{(2l+1) N_1}{\sum_{k=1}^{N_1} \left(\sum_{m=-l}^{l} \left| C_{l,m}^{k} \right| \right)} \right)^{\frac{N}{N_1^2}} \quad (65)$$

Ideally σ_{12} tends to 1 to obtain $F_2 = F_1$ and $D = 0$.

V. Conclusion and Future Work

In this work, we presented a new 3D shape descriptor, D.A.M.C-S.H.C. Direct and analytical method for calculating spherical harmonic coefficients and the indexing process provide a 3D shape descriptor robust to translation, rotation and scale variations. The D.A.M.C-S.H.C we developed has allowed us to present the efficiency of indexing the 3D objects in large databases, this global efficiency acting even for surfaces presented by a high density of points. It may be added that our descriptor satisfies the conditions created by the analysis of technical base models: the indexing process and robust and accurate research with very fast calculating of similarity.

Our future work concerns the correction term σ_{12}, solving the problem of identical objects with different numbers of points (refatization), either by increasing or decreasing the points for reference object and for different position of points.

References

[1] B. Cabral, N. Max and R. Springmeyer. Bidirectional Reflection Functions from Surface Bump Maps SIGGRAPH 273-281, 1987

[2] M. D'Zmura. Shading Ambiguity: Reflection and Illumination. In Computational Models of Visual Processing Landy and Movshon, eds., MIT Press, Cambridge, 187-207, 1991

[3] Ravi Ramamoorthi, Pat Hanrahan. An Efficient Representation for Irradiance Environment Maps SIG- GRAPH 497-500, 2001.

[4] B.K.P Horn. Extended Gaussian Images. Proc. of the IEEE, 72(12):1671–1686, dec. 1984.

[5] S.B. Kang and K. Ikeuchi. The complex EGI: a new representation for 3D pose determination. IEEE Trans. on Pattern Analysis and Machine Intelligence, 16(3):249–258, March 1994.21, hal-00538470, version 1 - 22 Nov 2010

[6] S. Hellam, Y. Oulahrir, F. El Mounchid, A. Sadiq, S. Mbarki "3D Objects Indexing Using Spherical Harmonic for Optimum Measurement Similarity" World Academy of Science, Engineering and Technology, International Journal of Computer, Information, Systems and Control Engineering Vol:9 No:1, 2015, pages 241-246.

[7] http://scienceblogs.de/mathlog/2011/09/30/topologie-von-flachen-clxxxvii/

[8] Ch. Brechbuhler, G. Gerig, and O. Kuhler, "Parametrization of Closed Surfaces for 3-D Shape Description", Computer Vision and Image Understanding, Vol. 61, No. 2, pp. 154-170, 1995.

[9] Gerig, G. Styner, M. Jones, D., Weinberger, D. Lieberman, J., 2001. Shape analysis of brain ventricles using spharm. In: MMBIA, pp. 171-178.

[10] T. Zaharia and F. Prêteux. 3D shape-based retrieval within the MPEG- 7 framework. In SPIE Conference 4304 on Nonlinear Image Processing and Pattern Analysis, volume XII, pp.133–145, San Jose, 2001.

[11] M. Kazhdan, B. Chazelle, D. Dobkin, T. Funkhouser, and S. Rusinkiewicz. A Reflective Symmetry Descriptor for 3D Models. Algorithmica (2004) 38: 201–225.

[12] R. Osada, T. Funkhouser, B. Chazelle, and D. Dobkin. Shape Distributions. ACM Trans. on Graphics, 21(4):807–832, oct. 2002.

[13] E. Wahl, G. Hillenbrand and G. Hirzinger. Surflet-pair-relation histograms: a statistical 3D-shape representation for rapid classification. In Proc. of 3-D Digital Imaging and Modeling 3DIM 2003. pp. 474–481, oct. 2003.

[14] R. Ohbuchi, T. Minamitani, and T .Takei. Shape-similarity search of 3D models by using enhanced shape functions. In Int. J. of Computer Applications inTechnology (IJCAT), 23(3/4/5):70-85, 2005.

[15] P. Papadakis, I. Pratikakis, S. Perantonis, and T. Theoharis. Efficient 3D Shape Matching and Retrieval using a Concrete Radialized Spherical Projection Representation. Pattern Recognition Journal, 40(9):2437–2452, Sept. 2007.

[16] M. Ben-Chen and C. Gostman. Characterizing Shape Using Confor- mal Factors. In Eurographics Workshop on 3D Object Retrieval, Crete, Greece, April 2008.

[17] T. Tung and F. Schmitt. The augmented multiresolution Reeb graph approach for content-based retrieval of 3D shapes. International Journal of Shape Modeling (IJSM), 11(1):91–120, June 2005.

[18] S. Biasotti, D. Giorgi, M. Spagnuolo, and B. Falcidieno. Reeb graphs for shape analysis and applications. Theoretical Computer Science, 392 (1-3):5–22, 2008.22 hal-00538470, version 1 - 22 Nov 2010

[19] N. Iyer, Y. Kalyanaraman, K. Lou, S. Jayanti, and K. Ramani. A Recon-figurable, Intelligent 3D Engineering Shape Search System Part I: Shape Representation. In ASME DETC'03, 23rd Computers and Information in engineering (CIE) Conf., Chicago, Illinois, 2003.

[20] S. Dietmar and V-V Dejan. 3d model retrieval with spherical harmonics and moments. In DAGM, pages 392–397. Springer-Verlag, 2001.

[21] D-V. Vranic. An improvement of rotation invariant 3d-shape based on functions on concentric spheres. In 2003 International Conference on Image Processing. ICIP. Proceedings, volume 3, pages III–757–60 vol.2, 2003. (Cited page 26.)

[22] J.W.H. Tangelder and R.C. Veltkamp, "A survey of content based 3D shape retrieval methods," Multimedia Tools and Applications, vol. 39, no. 3, pp. 441–471, Sept. 2008.

[23] T. Zaharia, F. Prêteux, "3D versus 2D/3D Shape Descriptors: A Comparative study", In SPIE Conf. on Image Processing: Algorithms and Systems, Vol. 2004, Toulouse, France, January 2004.

[24] M. Mousa, R. Chaine, and S. Akkouche. Frequency-based representation of 3d models using spherical harmonics. In WSCG'06 : Proceedings of the 14th International Conference in Central Europe on Computer Graphics, Visualization and Computer Vision, volume 14, pages 193–200, Plzen, Czech Republic, January 30 - February 3 2006.

[25] Peijiang Liu, Yunhong Wang, Zhaoxiang Zhang and Yiding Wang: automatic and robust 3d face registration using multiresolution spherical depth map, Proceedings of 2010 IEEE 17th International Conference on Image Processing, September 26-29, 2010, Hong Kong.

[26] Chao Wang, Yu-Shen Liua, Min Liue, Jun-Hai Yong, Jean-Claude Paul: Robust shape normalization of 3D articulated volumetric models, Computer-Aided Design 44 (2012) 1253–1268.

[27] W. E. Byerly. Spherical Harmonics, chapter 6, pages 195-218.New York: Dover, 1959. An elementary treatise on fouriers series and

spherical, cylindrical, and ellipsoidal harmonics, with applications to problems in mathematical physics.
[28] Mathematical formulas and tables, M. R. SPIEGEL, Rensselaer Polytechnic Institute, 1968.
[29] Mary L. Boas Mathematical methods in the physical sciences, second edition, 1996.
[30] Abramowitz, M. and I. S. Stegun, Handbook of Mathematical Functions, Dover Publications, Inc., NewYork, NY, 1965.
[31] Andrews, L. C., Special Functions for Engineers and Applied Mathematicians, MacMillan PublishingCo. New York, NY. 1985.
[32] K.T. Tang, Mathematical Methods for Engineers and Scientists 3, springer, 2007.
[33] I.S. Gradshteyn and I.M. Ryzhik, Alan Jeffrey, Editor, Table of Integrals, Series, and Products Seventh Edition, 2007.
[34] H. Alzer, On some inequalities for the gamma and psi functions, Mathematics of Computation, Volume 66, Number 217, January 1997.